Supporting Information

Structural transformation in vesicles upon hydrolysis of phosphatidylethanolamine and phosphatidylcholine with phospholipase C

Wye-Khay Fong[a,b,c*], Antoni Sánchez-Ferrer[a], Michael Rappolt[d], Ben J. Boyd[b] and Raffaele Mezzenga[a*]

[a]ETH Zürich, Department of Health Sciences & Technology, 8092 Zürich, Switzerland; [b]Drug Delivery, Disposition & Dynamics, Monash Institute of Pharmaceutical Sciences, Monash University, 381 Royal Parade, Parkville, Victoria 3052, Australia. [c]Adolphe Merkle Institute, University of Fribourg, Chemin des Verdiers 4, 1700 Fribourg, Switzerland. [d]School of Food Science and Nutrition, University of Leeds, LS2 9JT, United Kingdom.

[*]Raffaele.mezzenga@hest.ethz.ch & khay.fong@newcastle.edu.au

Structural Analysis of the Lamellar and Inverse Hexagonal Phase

1. Bilayer Thickness Determination by Fourier Analysis

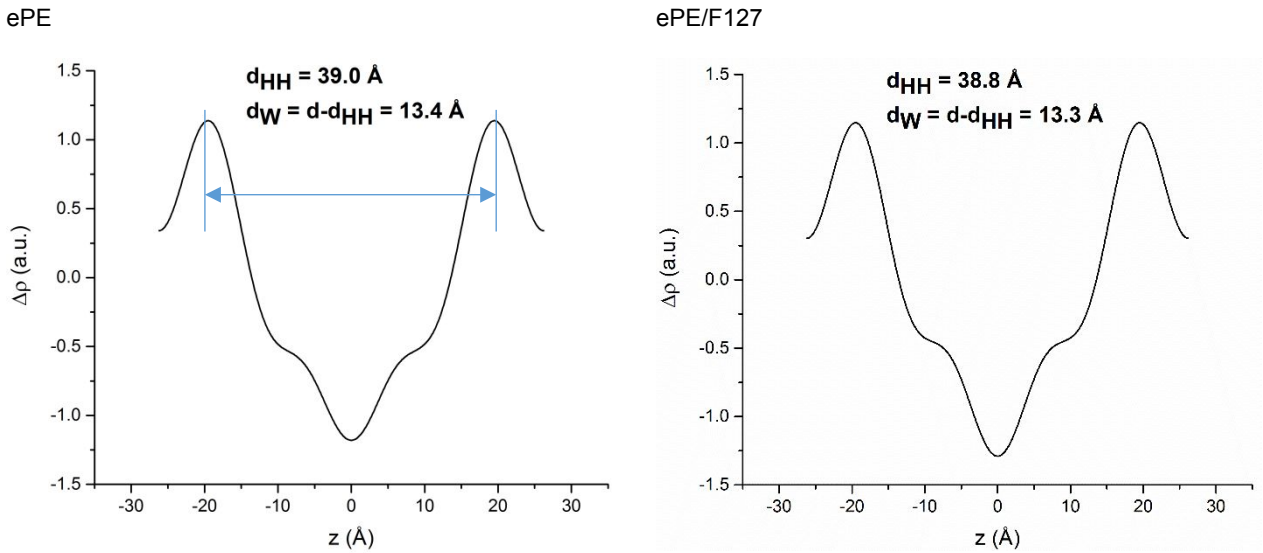

Figure SI-1. The electron density profiles (EDPs) as determined by Fourier analyses of the bilayer stack. The head-to head group distance is determined form the position of the EDP maxima (blue double arrow). For methodological details, refer to the review.[1]

2. Estimation of Bilayer Thicknesses Applying a "2-Peak" and the Luzzati Method

In a previous publication, we demonstrated diffraction data can be exploited to gain an estimate of the bilayer thickness, when only the first 2 diffraction orders are at hand.[2] It relies on good *a priori* knowledge of three structural bilayer parameters, *i.e.*, the head-group extension, σ_H, the methyl trough extension, σ_C, and relative electron density of the methyl trough to head-group regions, ρ_R (for precise definitions see [2]). A literature survey on various PC and PE bilayers systems revealed that these particular bilayer parameters do not vary much and resulted in the mean values of σ_H = 3.1 ± 0.3 Å, σ_C = 4.4 ± 0.5 Å, and ρ_R = 0.9 ± 0.1.[2] Using these material parameters for our sPC data and the experimentally determined form factor values of the first and second order diffraction peaks (F_1 and F_2, respectively), the head- to head-group distance can be estimated from

$$d_{HH} = d \cdot \phi_L \tag{6}$$

where the lipid volume fraction Φ_L in this "2-peak" method depends on F_1/F_2, σ_H, σ_C and ρ_R (for more details and discussion see references[2-3]). Note, we preferred this method to global fitting techniques,[4] since we were mainly interested in the overall bilayer thickness trends, and further, some of the data displayed clear phase-coexistence regimes with micellar scattering contributions (see Fig. 4), that complicates the appropriate application of global fitting methods.

As a comparison to bilayer determination from the EDPs and estimations above (Eq. 1), the bilayer thickness (water thickness) of L_α phases were also derived from the Luzzati method[5] and are displayed in Table SI-1. Presuming full hydration of the phospholipid headgroups, specifically 23 water molecules per PC and 12 water molecules per PE headgroup as reported by McIntosh *et al.*,[6] the thickness of water between lamellae (d_W) and the lipid length (d_L) was calculated according:

$$d_W = d \cdot \phi_W \tag{7}$$

$$d_L = \frac{1}{2} d \cdot (1 - \Phi_W) \tag{8}$$

where Φ_W refers to the volume fraction of water.

Table SI-1. Lattice parameter (d), water thickness ($d_{W\,Luz}$) and lipid length (d_L) are compared to $d_{HH}/2$ and $dw = d - d_{HH}$ determined from the 2-peak method (PC-samples) and the FT analysis (PE-samples). All samples are in the L_α phase.

	sPC	sPC/F127	ePE	ePE/F127
d (Å)	62.3	58.5	52.5	52.4
d_L (Å)	19.8	18.6	20.1	20.1
$d_{W\,Luz}$ (Å)	22.8	21.3	12.2	12.2
$d_{HH}/2$ (Å)	18.7	19.4	19.5	19.4
d_W (Å)	24.9	19.7	13.4	13.4

We note, that while the Luzzati method does not consider water penetrating into the bilayer region, which leads to a systematic underestimation of the true steric bilayer thickness,[7] for most common phospholipids in the fluid phase, $2d_L$ can be approximately identified with the head- to head-group distance, d_{HH}.[7] This is well confirmed for the PE-data,

in which the hydration properties are not expected to vary much, while stronger deviations are observed for the sPC-samples, since a constant hydration of 23 water molecules per PC is not realistic, in particular for the swollen sPC sample.

3. Definition of Structural Parameters in the Inverse Hexagonal Phase

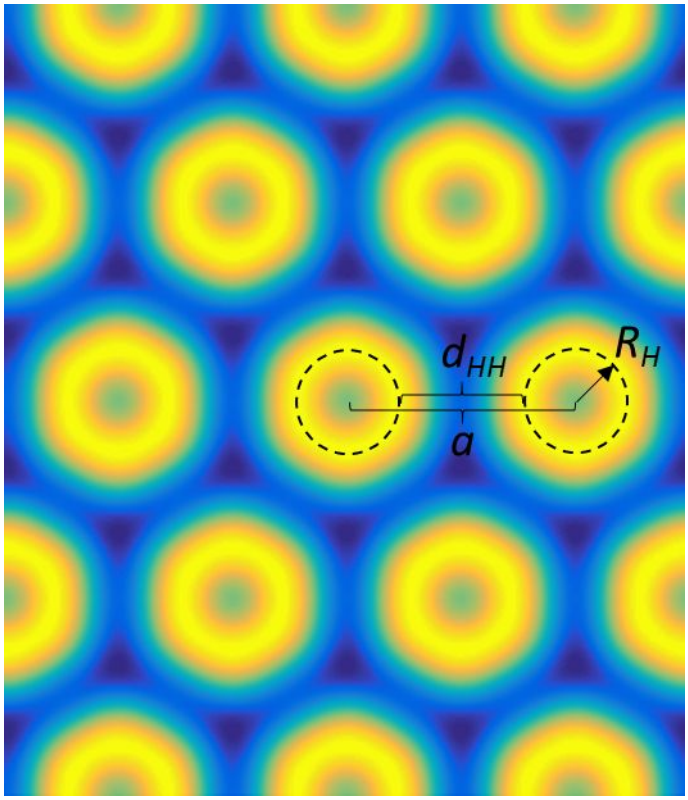

Figure SI-2. The electron density map of the inverse hexagonal phase of ePE F127 at t = 736 s (compare Figure 2 bottom). High electron densities are color-coded in yellow (head group positions) and low densities in dark blue (methyl trough regions). The unit cell parameter, a, the smallest head to head group distance, d_{HH} and the medium radius to the head group position R_H are defined for clarity in the electron density map. For more details refer to the Materials and Methods section.

Nuclear Magnetic Resonance (NMR) Spectra

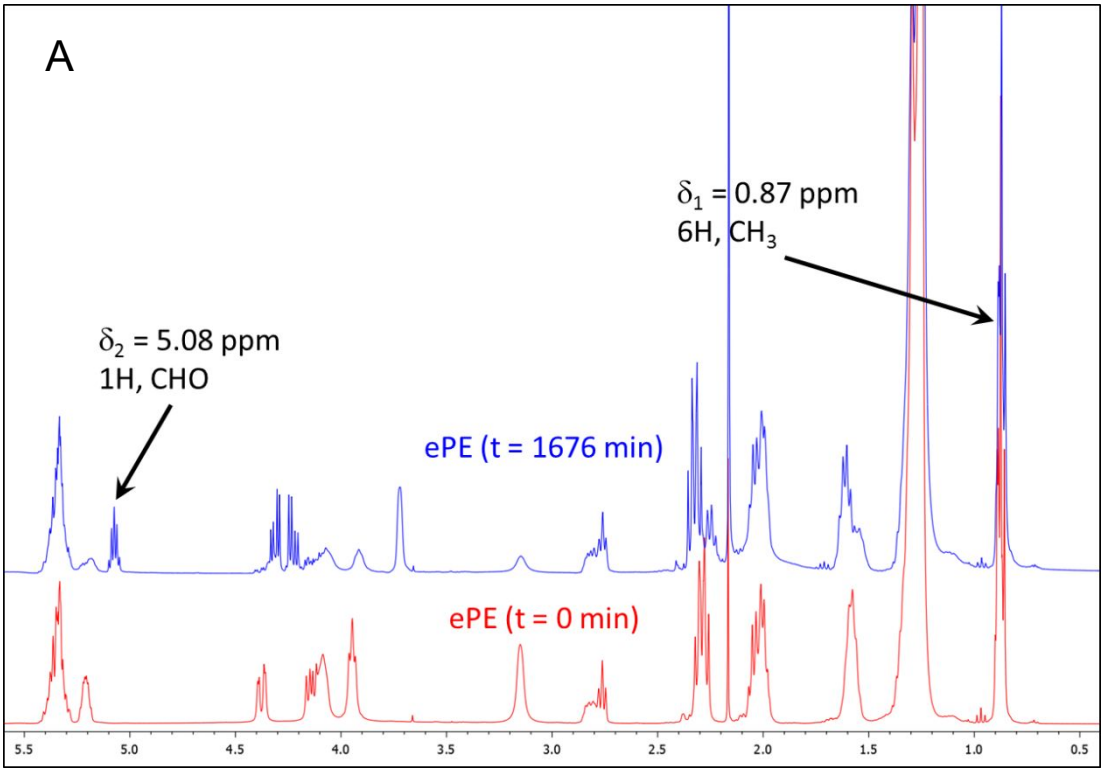

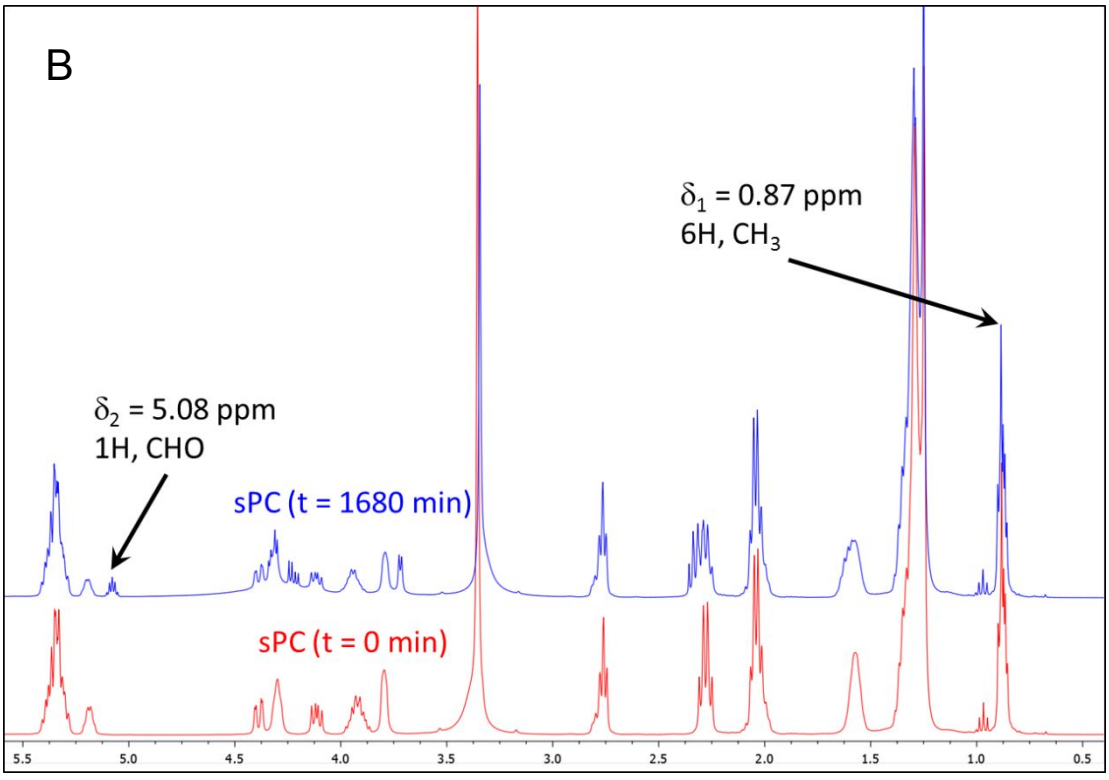

Figure SI-3. A. ^{1}H NMR spectra for the ePE before (red curve) and after hydrolysis (blue curve), showing the apparition of the peak at 5.08 ppm corresponding to the proton in C2 of the glycerine moiety. B. ^{1}H NMR spectra for the sPC before (red curve) and after hydrolysis (blue curve), showing the apparition of the peak at 5.08 ppm corresponding to the proton in C2 of the glycerine moiety.

Particle Size Distribution as Measured by Dynamic Light Scattering (DLS)

Particle size distribution (Z-average) and polydispersity index (PDI) of the lipid dispersions were determined by dynamic light scattering using Zeta Sizer Nano-series (Nano ZS, Malvern, Switzerland). Samples were taken at time 0 and 24 h and were subsequently diluted (3000-fold) with milliQ water and measured at 37 ± 0.5 °C in triplicate.

Table SI-2. The hydrodynamic diameter (d) and polydispersity index (PDI) of lipid particles at time 0 and after 60 min.

Time (min)	ePE/F127		sPC/F127	
	d (nm)	PDI	*d* (nm)	PDI
0	133.8	0.346	174.3	0.476
60	1188	0.989	1101	1

Structural transformations of ePE

A - ePE/F127, without PLC.

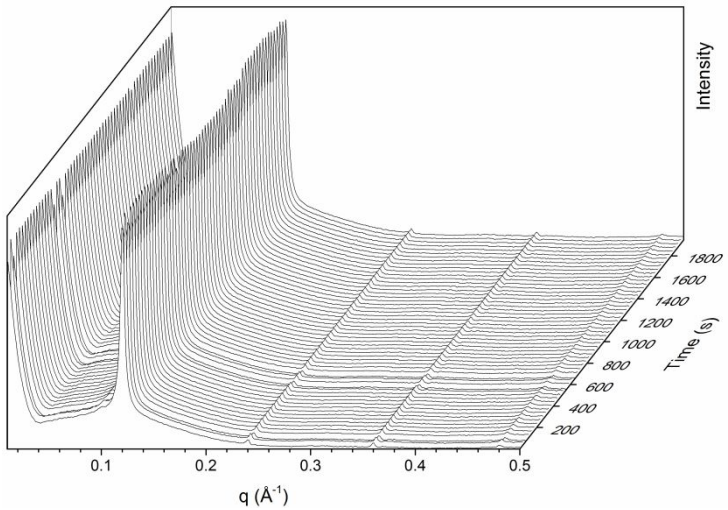

B - ePE/F127, hydrolysis with PLC.

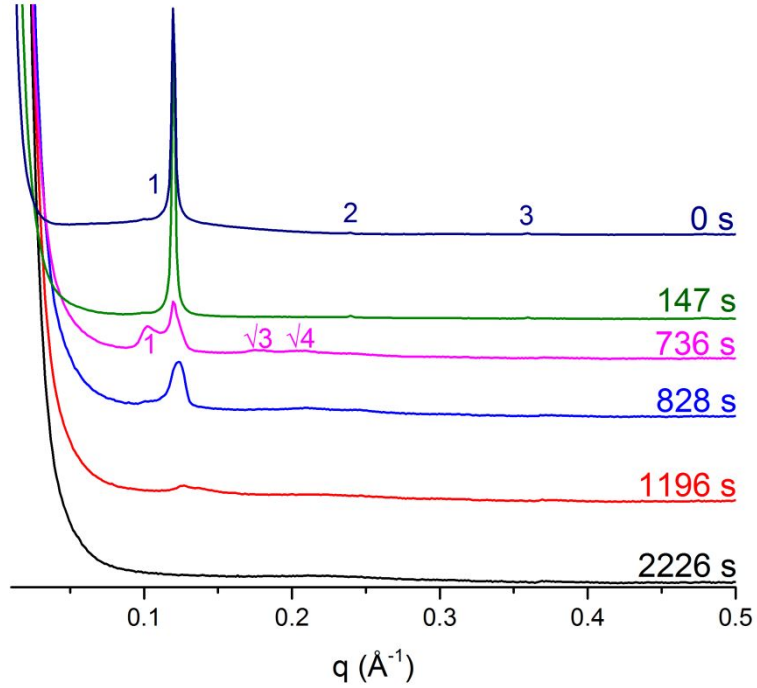

C - ePE, hydrolysis with PLC.

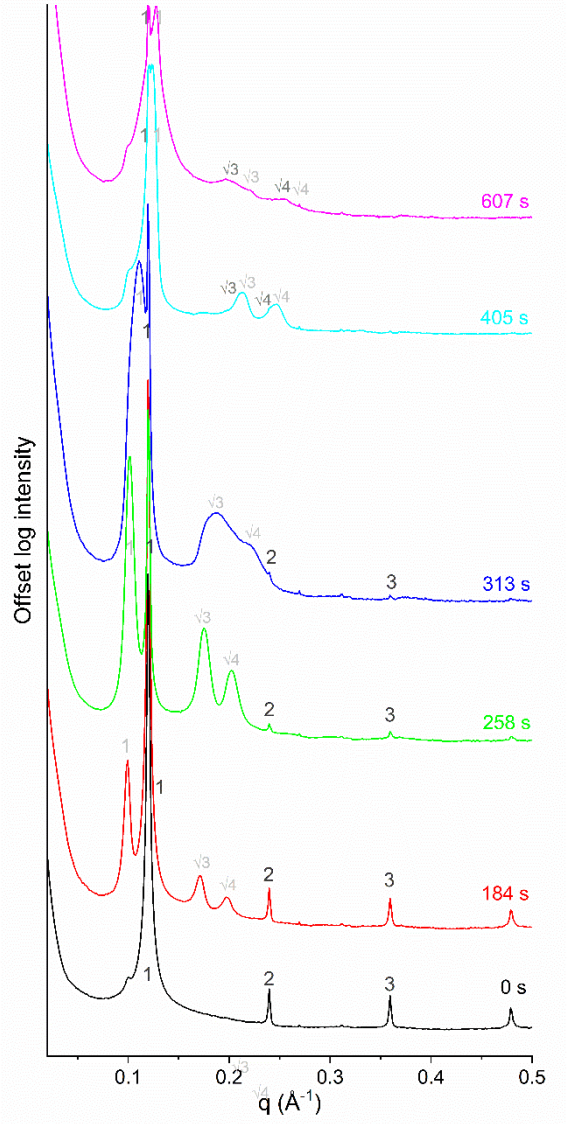

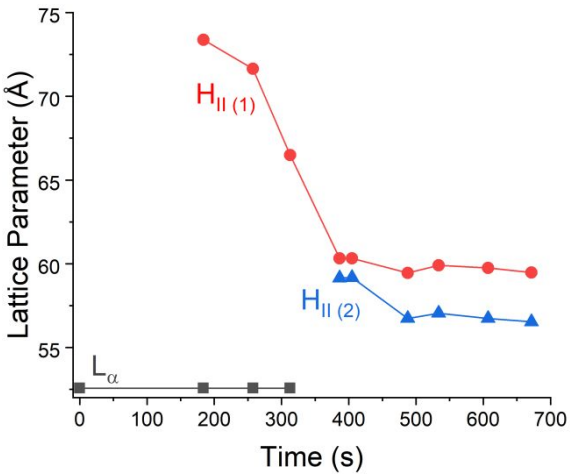

Figure SI-4. Time resolved SAXS scattering profiles of ePE formulations. Temporal evolution of the SAXS scattering curves for (A) dispersion containing ePE/F127 without PLC; Selected SAXS patterns highlighting phase transitions during the PLC catalysed hydrolysis of (B) ePE/F127; (C) Selected SAXS patterns highlighting phase transitions during the PLC catalysed hydrolysis of ePE and a plot of lattice parameter over time showing the evolution of H_{II} phases.

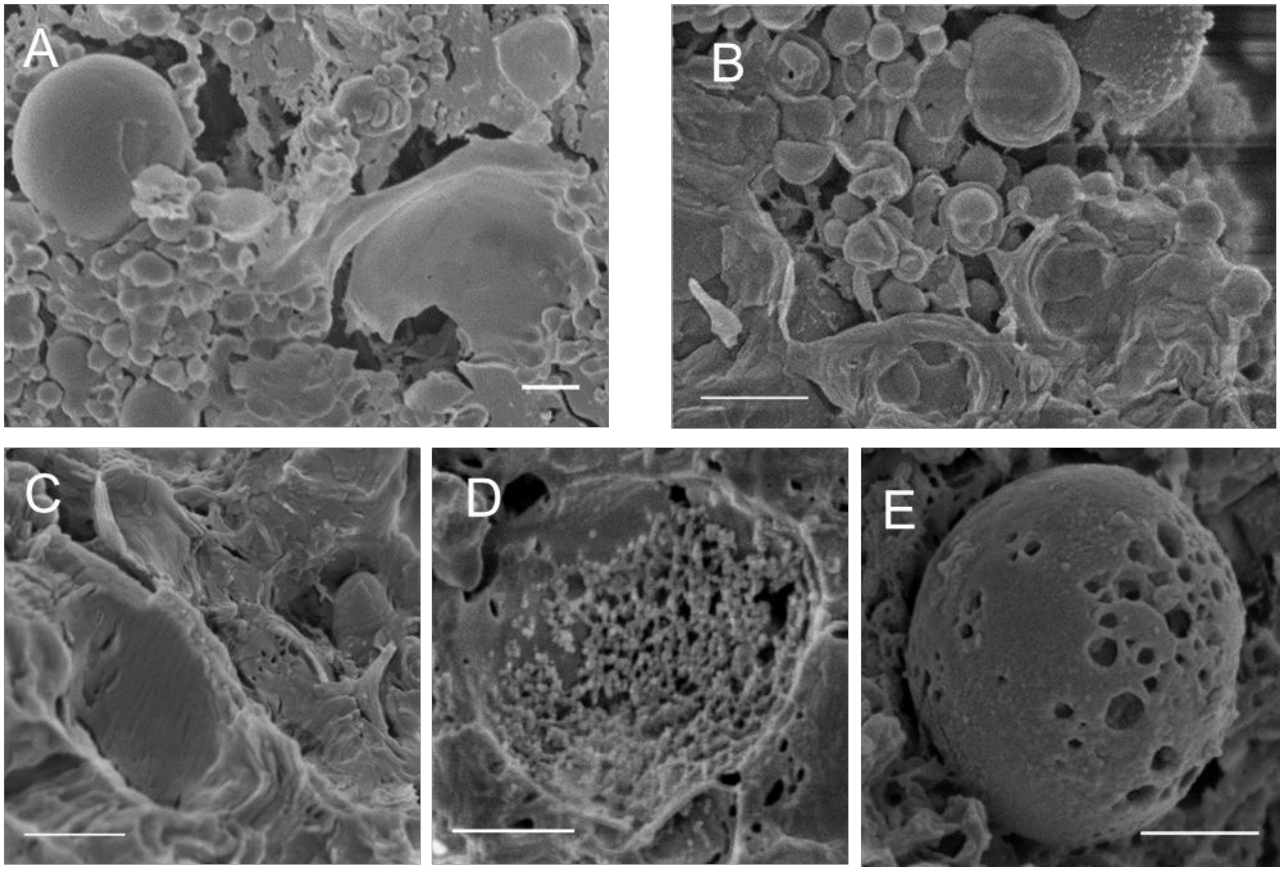

Figure SI-5. CryoSEM images displaying the progression of the hydrolysis of ePE/F127 catalysed by PLC displayed at 30 s (A), 315 s (B), 611 s (C), 1800 s (D) and 3610 s (E). Scale bars = 500 nm.

Structural transformations of sPC

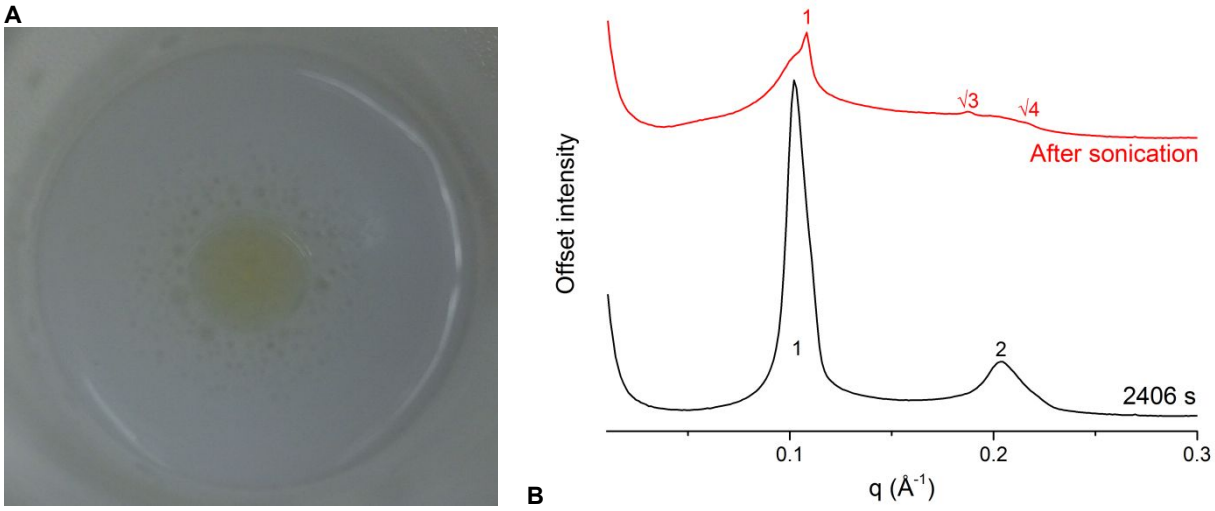

Figure SI-6. A. Top view of PLC catalysed hydrolysis of sPC after 1 h demonstrating clear phase separation of the oil phase (DAG4) from the dispersion. B. SAXS scattering profiles of the PLC catalysed hydrolysis of sPC vesicles after 2406 s and after 5 min of probe ultrasonication. The input of energy into the mixture results in the development of a H_{II} phase attributed to the re-assembly of the produced DAG4 into the sPC bilayer.

The hydrolysis of sPC with phospholipases D (PLD) and phospholipases A2 (PLA2) also progressed without a change in nanostructure (Fig SI-7). As the hydrolysis of the headgroup of the sPC to form a phosphatidic acid and choline progresses, there is an observed decrease in the intensity of the lamellar signal; however, there is no change in nanostructure in the experimental conditions in terms of pH and ionic strength. The action of PLD on a sPC-based lipidic bilayer imparts a negative charge upon the system,[8] however, this does not seem to have an effect on membrane curvature in this case, in part attributed to the fact that phosphatidic acids themselves self-assemble into lamellar structures in aqueous dispersions (Fig. SI-7). This is in agreement with recent studies utilising molecular dynamics simulations that found that the produced phosphatidic acid takes part in ion coordination in phospholipid bilayers without altering structure.[9] Consistent with this, the action of PLA2 results in the formation of a single chained phospholipid, which also promotes the formation of lamellar phases;[10] thus, it follows that the hydrolysis of sPC with PLA2 does not result in the formation of inverse phases.

A - PLD catalysed hydrolysis of sPC.

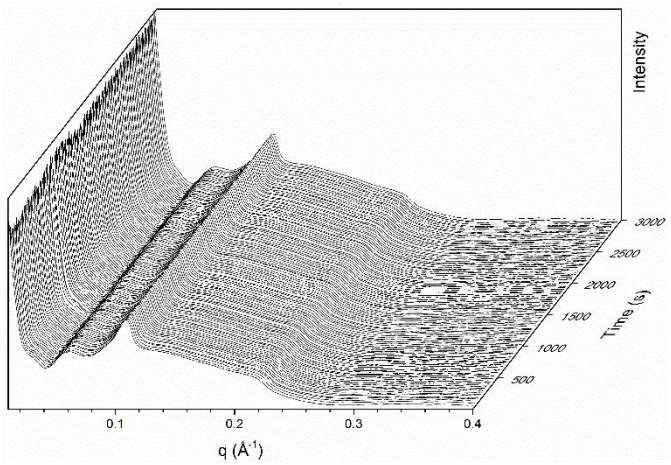

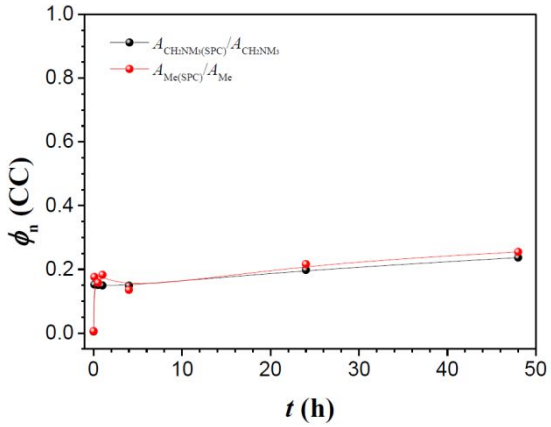

B - PLA2 catalysed hydrolysis of PC,

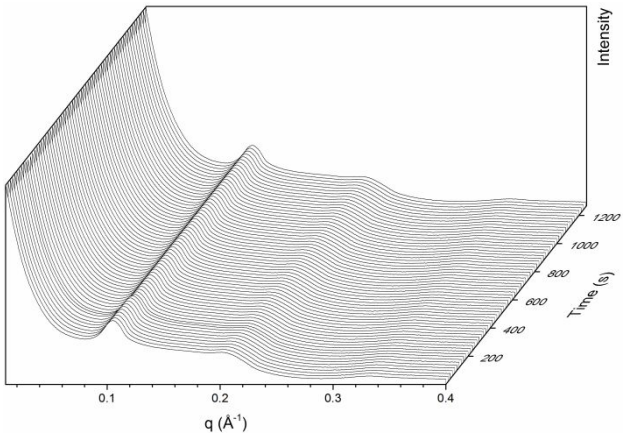

C - PLC catalysed hydrolysis of DSPA-Na.

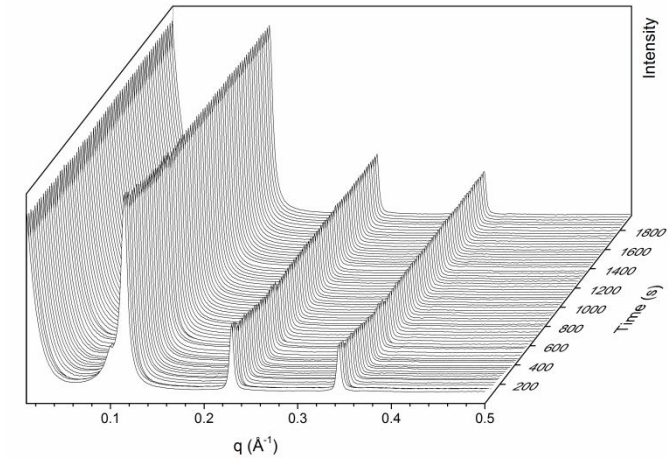

Figure SI-7. Time-resolved SAXS scattering profiles showing (A) the evolution of structure of a dispersion containing sPC/F127 with PLD, where the quantification of hydrolysis of the PC molecules are followed via ^{1}H NMR (right); B. PLA2 catalysed hydrolysis of sPC; and C. PLC catalysed hydrolysis of DSPA-Na.

Representative Cryo-SEM Images

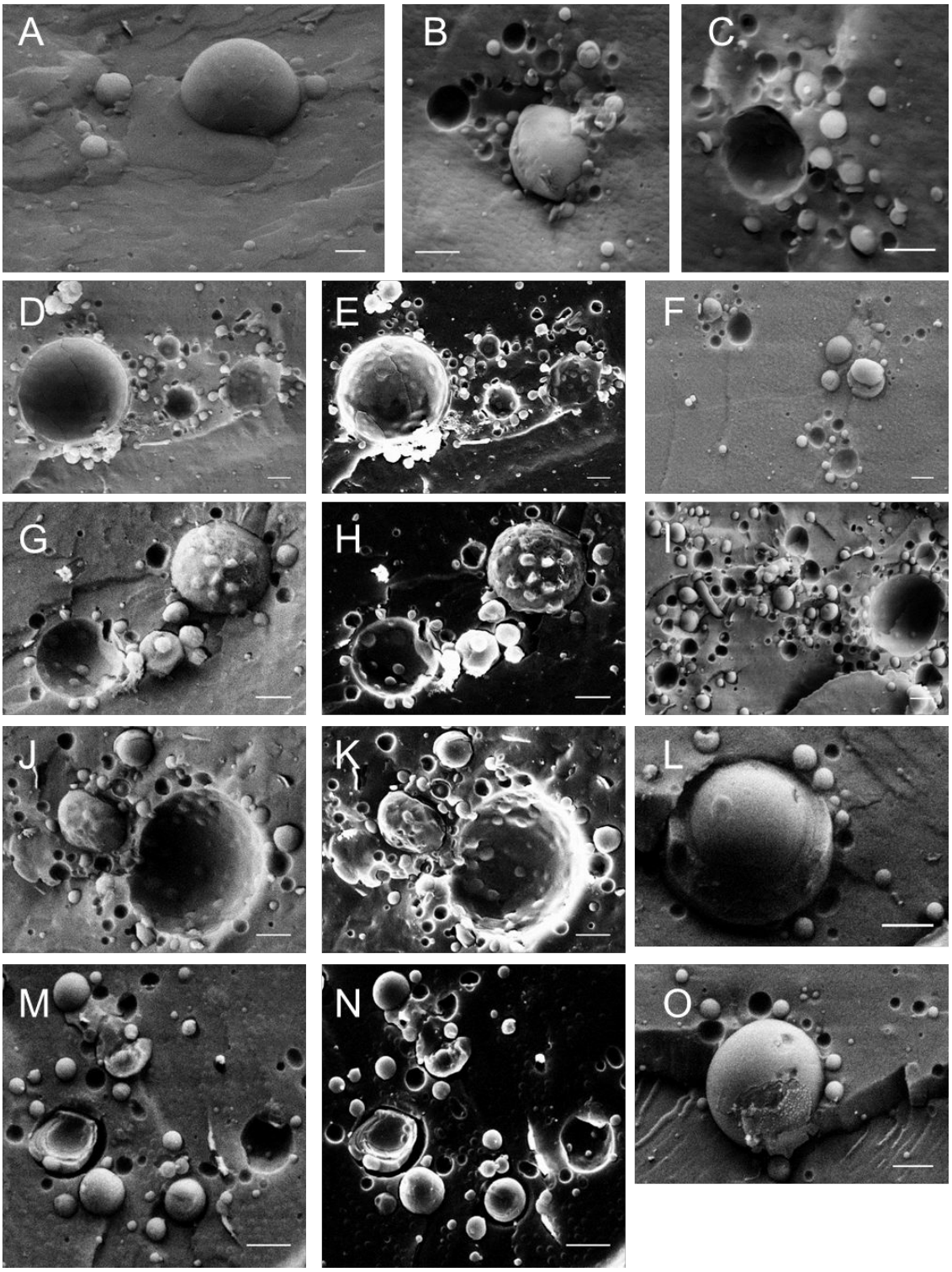

Figure SI-8. CryoSEM images displaying the progression of the hydrolysis of sPC/F127 catalysed by PLC displayed at 10 s (A), 364 s (B, C), 680 s (D-F), 1935 s (G-I) and 3630 s (J-O). Scale bars = 500 nm.

Molecular simulations

Structures were drawn and simulated using ChemDraw and Chem3D Ultra v16.0.1.4 software, and the molecular mechanics force field (MMFF) method together with the Allinger's mining minima (MM2) algorithm with a root-mean-square (RMS) gradient of 0.01 kcal·Å^{-1}·mol^{-1} was used for the geometrical optimisation of the molecules by minimising the energy of the system and taking into account hydrogen bonding, ions-dipole and Van der Waals interactions.

a) b)

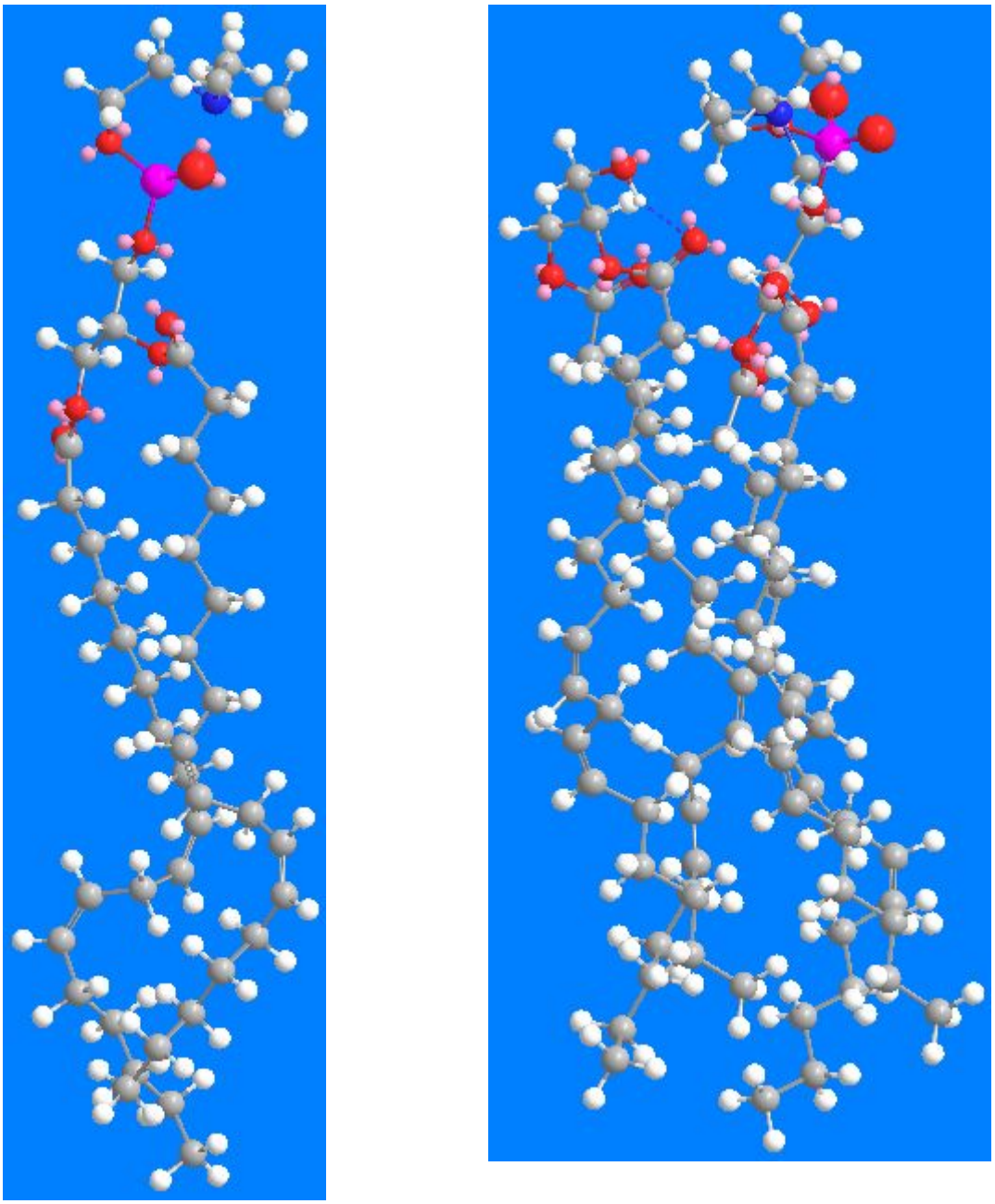

Figure SI-9: a) MM2 simulation for the sPC molecule alone showing no intra-hydrogen bonding. b) MM2 simulation for the sPC molecule in the presence of a DAG4 molecule showing no inter-hydrogen bonding.

a)

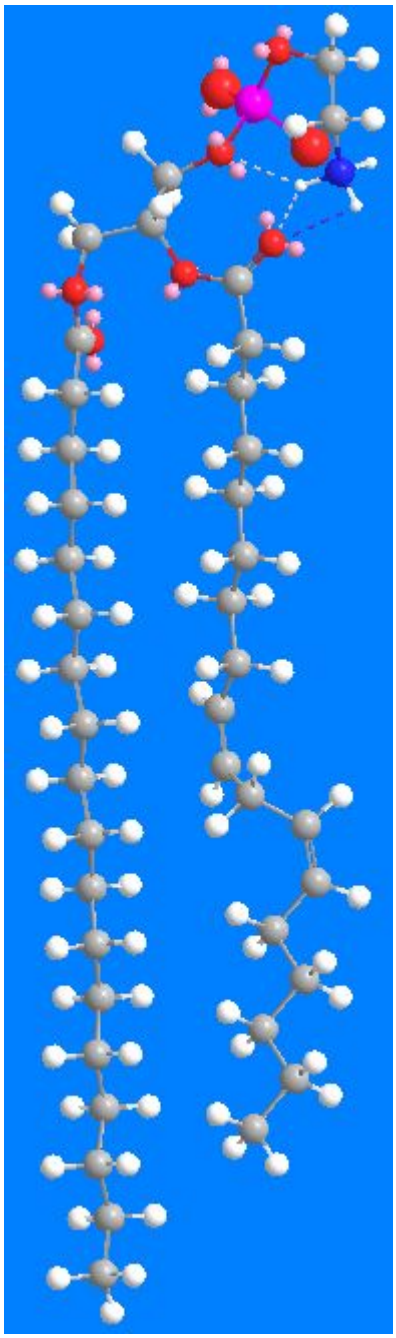

b)

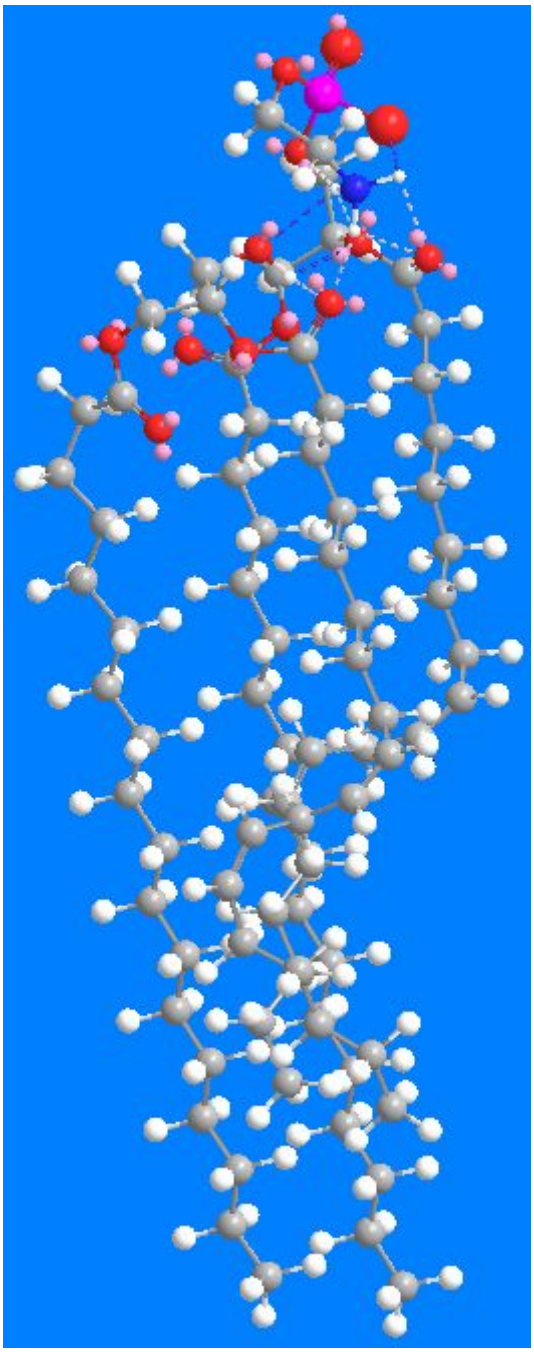

Figure SI-10: a) MM2 simulation for the ePE molecule alone showing intra-hydrogen bonding. b) MM2 simulation for the ePE molecule in the presence of a DAG1 molecule showing inter-hydrogen bonding.

References

1. Li, N. Y. D.; Perutkova, S.; Iglic, A.; Rappolt, M., My first electron density map: A beginner's guide to small angle X-ray diffraction. *Elektrotehniški vestnik* **2017,** *84* (3), 69-75.
2. Rappolt, M., Bilayer thickness estimations with "poor" diffraction data. *J Appl Phys* **2010,** *107* (8).
3. Rappolt, M., Chapter One - 50 Years of structural lipid bilayer modelling. In *Advances in Biomembranes and Lipid Self-Assembly*, Iglič, A.; Rappolt, M.; García-Sáez, A. J., Eds. Academic Press: 2019; Vol. 29, pp 1-21.
4. Heftberger, P.; Kollmitzer, B.; Heberle, F. A.; Pan, J.; Rappolt, M.; Amenitsch, H.; Kucerka, N.; Katsaras, J.; Pabst, G., Global small-angle X-ray scattering data analysis for multilamellar vesicles: the evolution of the scattering density profile model. *J Appl Crystallogr* **2014,** *47* (1), 173-180.
5. Luzzati, V.; Husson, F., The structure of the liquid-crystalline phases of lipid-water systems. *The Journal of Cell Biology* **1962,** *12* (2), 207-219.
6. McIntosh, T. J., Hydration properties of lamellar and non-lamellar phases of phosphatidylcholine and phosphatidylethanolamine. *Chem. Phys. Lipids* **1996,** *81* (2), 117-131.
7. Nagle, J. F.; Tristram-Nagle, S., Structure of lipid bilayers. *Biochim. Biophys. Acta, Rev. Biomembr.* **2000,** *1469* (3), 159-195.
8. Liu, C.; Huang, D.; Yang, T.; Cremer, P. S., Monitoring Phosphatidic Acid Formation in Intact Phosphatidylcholine Bilayers upon Phospholipase D Catalysis. *Anal. Chem.* **2014,** *86* (3), 1753-1759.
9. Holme, M. N.; Rashid, M. H.; Thomas, M. R.; Barriga, H. M. G.; Herpoldt, K. L.; Heenan, R. K.; Dreiss, C. A.; Bañuelos, J. L.; Xie, H.-n.; Yarovsky, I.; Stevens, M. M., Fate of Liposomes in the Presence of Phospholipase C and D: From Atomic to Supramolecular Lipid Arrangement. *ACS Cent. Sci.* **2018,** *4* (8), 1023-1030.
10. Fong, W. K.; Hanley, T. L.; Thierry, B.; Tilley, A.; Kirby, N.; Waddington, L. J.; Boyd, B. J., Understanding the photothermal heating effect in non-lamellar liquid crystalline systems, and the design of new mixed lipid systems for photothermal on-demand drug delivery. *Phys Chem Chem Phys* **2014,** *16* (45), 24936-24953.